

# Computational Model of the Anode of a $\text{Zn}-\text{MnO}_2$ Battery

Gokhale, Patel, and Li

December 2019

## 1 Introduction

Energy production by renewable energies i.e. winds or solar power is fluctuating. Therefore special efforts are required to match energy production and consumption. Traditional power plants are not ideal to compensate for energy fluctuations, especially because renewable energies are strongly decentralized. Furthermore, portable electronic devices and electro-mobility rely on compact energy storage devices. Battery Technology is fast emerging as the champion in the sustainable energy revolution. Zinc Anode AA batteries have made unparalleled progress, in today's Alkaline battery world, but there are still some major voids to be filled.

Growth and advances in the portable electronic industry require commercial alkaline  $\text{Zn}/\text{MnO}_2$  AA batteries to function under high power and high drain conditions. Unfortunately AA Batteries operate inefficiently at high drain rates. For example the run-time of a AA battery at 1000 mA continuous drain rate is typically less than 20% of that discharged at 10 mA. This inefficiency is due to various heat losses and due to severe polarization across the Zn (anode) and  $\text{MnO}_2$  (cathode) electrodes at high drain rates.

## 2 Structure of Battery

The  $\text{Zn}/\text{MnO}_2$  AA cell has a bobbin-type construction where both electrodes are porous as shown in Fig 1.

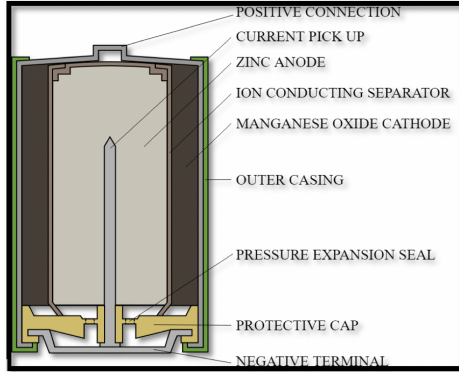


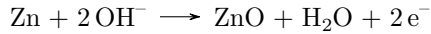
Figure 1: Structure of  $Zn/MnO_2$  cell

The anode consists of zinc powder that is usually suspended in gelled electrolyte of concentrated KOH in water, and the cathode includes a physical mixture of electrolytic manganese dioxide and graphite.

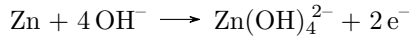
### 3 Chemistry and Working

The chemistry inside the battery is an oxidation and reduction reaction. The chemistry inside a battery is an oxidation-reduction reaction. The oxidation of zinc proceeds by a dissolution precipitation process which is the acceptance of electrons, forming an ion and then precipitating on saturation, while  $MnO_2$  is reduced by a solid state intercalation of  $H^+$  ions into the  $MnO_2$  lattice.

#### Anode:



#### Dissolution:



#### Precipitation:



As shown in Fig 2. the cathode connects to the positive end of the battery where electrons leave and the anode is connected to the negative end of the battery where electrons enter the battery. The ions inside the battery react with the electrodes thus completing the circuit.

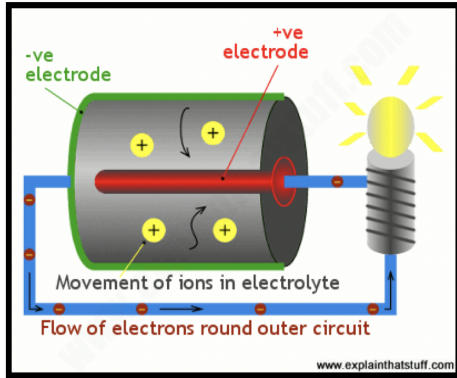


Figure 2: Working of Cell

#### 4 In depth of Anode

It was described above when the first dissolution occurs, and the concentration of the zincate ion surpasses its equilibrium value, the precipitation of the zinc oxide ( $ZnO$ ) transpires. It would form the product of  $ZnO$  and reactant  $Zn$ , which produces two independent stages, compared to the cathode.

The equations for the concentration of hydroxyl ion and zincate ion derived by substituting the stoichiometric coefficients into the generalized expressions.

The Butler-Volmer type of relation is used to describe the electrochemical rate of the anode, as shown below.

$$j_{anode} = \left( \frac{\partial i_2}{\partial r} + \frac{i_2}{r} \right) = \\ a_a i_{o,ref,a} \left[ \left( \frac{C_{Zn(OH)_4^{-2},s}}{C_{Zn(OH)_4^{-2},ref}} \right)^{0.06} \left( \frac{C_{OH^-,s}}{C_{OH^-,ref}} \right)^{2.59} e^{(1-\alpha_a)2F\eta/RT} \right. \\ \left. - \left( \frac{C_{Zn(OH)_4^{-2},s}}{C_{Zn(OH)_4^{-2},ref}} \right)^{0.94} \left( \frac{C_{OH^-,s}}{C_{OH^-,ref}} \right)^{-0.92} e^{-\alpha_a 2F\eta/RT} \right]$$

Initial conditions define the reference conditions. Considering the mass transport effects, the concentrations of anions can be analyzed.

$$C_{OH^-,s} = C_{OH^-} - \left( \frac{\partial i_2}{\partial r} + \frac{i_2}{r} \right) \frac{1}{2Fa_a K_{KOH}}$$

$$C_{Zn(OH)_4^{-2},s} = C_{Zn(OH)_4^{-2}} + \left( \frac{\partial i_2}{\partial r} + \frac{i_2}{r} \right) \frac{1}{2Fa_a K_{K_2Zn(OH)_4}}$$

The mass transfer coefficients  $K_{KOH}$  and  $K_{K_2Zn(OH)_4}$  are defined by Sunu and Bennion for the zinc electrode.

$$a_i K_i = K_i^0 \frac{a_a - a_m}{\ln(\frac{a_a}{a_m})}, i = KOH, K_2Zn(OH)_4$$

By assuming ideal spherical shape of zinc particle and a given initial condition, the interfacial area,  $a_a$ , can be calculated.

$$a_a = a_a^0 \left( \frac{1 - \epsilon_a}{1 - \epsilon_a^0} \right)^{2/3}$$

The reaction available area,  $a_m$ , can also be calculated as follows

$$a_m = a_a \frac{\epsilon_{Zn}^{2/3}}{\epsilon_{Zn}^{2/3} + (\epsilon_{ZnO} + \epsilon_{Hg})^{2/3}}$$

where  $\epsilon_i$  ( $i = Zn, ZnO$  or  $Hg$ ) are the volume fractions. According to Faraday's law applied in reaction at each time step, the volume fraction of Zn can be determined. Furthermore, the volume fraction of ZnO is the difference between the electrode porosity and  $\epsilon_{Zn}$ .

The rate constant  $K_s$ , is influenced by the mass transport of zincate due to the changing particle size.

$$\frac{1}{K_s} = \frac{1}{\frac{a_m K_{K_2Zn(OH)_4}}{\ln[a_a/(a_a - a_m)]}} + \frac{1}{\frac{(a_a - a_m)}{a_a} k_x}$$

The cell overpotential equation for the anode describes the ternary electrolyte. The reference condition is chosen as the same composition as the anode,

$$\begin{aligned} \frac{\partial \eta}{\partial r} &= i_2 \left[ \frac{1}{\epsilon_a^{1.5} \kappa} + \frac{1}{\sigma} \right] - \frac{I}{2\pi r L \sigma} \\ &+ \frac{2RT}{F} \left[ 2 - t_{OH^-}^* \right] \left( \frac{1}{C_{OH^-} f_{\pm, KOH}} \right) \frac{\partial f_{\pm, KOH} C_{OH^-}}{\partial r} \\ &+ \frac{3RT}{F} \left[ -\frac{1}{2} + \frac{t_{Zn(OH)_4^{-2}}^*}{-2} \right] \left( \frac{1}{C_{Zn(OH)_4^{-2}} f_{\pm, K_2Zn(OH)_4}} \right) \frac{\partial f_{\pm, K_2Zn(OH)_4} C_{Zn(OH)_4^{-2}}}{\partial r} \end{aligned}$$

By assuming the zincate ion is always present in the anode, the binary electrolyte overpotential equations can be neglected.

$$\sigma = \sigma_{Zn} \epsilon_{Zn}^{1.5} + \sigma_{ZnO} \epsilon_{ZnO}^{1.5} + \sigma_{Hg} \sigma_{Hg}^{1.5}$$

The effective matrix conductivity,  $\sigma$ , is determined by considering parallel conduction paths and reflects the conductivity of the zinc, ZnO and mercury,

The expression for the volume average velocity is given as,

$$\begin{aligned} \frac{\partial \epsilon_a}{\partial t} + \left( \frac{\partial v^*}{\partial r} + \frac{v^*}{r} \right) = & \left[ \bar{V}_{KOH}(2t_{OH^-}^* - 4) + \bar{V}_{K_2Zn(OH)_4} \frac{(2t_{Zn(OH)_4}^* + 2)}{2} \right] \\ & \left( \frac{\partial i_2}{\partial r} + \frac{i_2}{r} \right) \frac{1}{2F} + a_a k_s (C_{Zn(OH)_4}^* - C_{OH^-}^2 / K_{eq}) \\ & (2\bar{V}_{KOH} + \bar{V}_{H_2O} - \bar{V}_{K_2Zn(OH)_4}) \end{aligned}$$

and the porosity expression is,

$$\frac{\partial \epsilon_a}{\partial t} = \frac{\bar{V}_{Zn}}{2F} \left( \frac{\partial i_2}{\partial r} + \frac{i_2}{r} \right) - a_a k_s (C_{Zn(OH)_4}^* - C_{OH^-}^2 / K_{eq}) \bar{V}_{ZnO}$$

## 5 Initial and Boundary Conditions

### Boundary Conditions

**Anode Current Collector,  $r = r_{ac}$**

$$\partial C_{OH^-} / \partial r = 0$$

$$\partial C_{Zn(OH)_4}^* / \partial r = 0$$

$$i_2 = 0$$

$$\partial i_2 / \partial r + i_2 / r = j_{anode}(\eta)$$

$$v^* = 0$$

**Anode-Separator,  $r = r_a$**

$$\epsilon_g^{1.5} \partial C_{OH^-} / \partial r|_{sep} = \epsilon_a^{1.5} \partial C_{OH^-} / \partial r|_{anode}$$

$$\epsilon_g^{1.5} \partial C_{Zn(OH)_4}^* / \partial r|_{sep} = \epsilon_a^{1.5} \partial C_{Zn(OH)_4}^* / \partial r|_{anode}$$

$$i_2 = I/(2\pi Lr)$$

$$\partial i_2 / \partial r + i_2 / r = j_{anode}(\eta)$$

$C_{OH^-}$ ,  $C_{Zn(OH)_4}^*$ , and  $v^*$  are continuous

Figure 3: Boundary conditions

For initial conditions, the flux of all the particles in the cell are equal to zero. The flux combines migration, convection and diffusion. At initial state, the current density is considered as zero so that migration flux can be neglected. Besides, in the cell, there is no convection because of still solution. As assuming, the electrolyte distributing evenly, there is no diffusion. At the internal

boundaries the concentration, volume average velocity and species flux must be continuous. Continuous means that their values are continuously changing i.e they depend on the flux of  $\text{OH}^-$  ions from the cathode At this condition, the solution current density is completely ionic since electrons do not pass through the separator.

In order to incorporate continuous boundary conditions, a partial cathode model was programmed assuming the electrode to be planar and having uniform current density. The flux of  $\text{OH}^-$  ions can then be governed and controlled by the extent of reaction since that determines the amount of hydroxyl ions produced in the cathode.

## 6 Anode Model

The anode model was built off of nonlinear equations which is solved by using the finite difference technique. Finite difference methods are numerical methods for solving differential equations with boundary values, in which the finite differences approximate the derivatives. Finite difference methods are discretization methods for boundary value and initial value problems.

In order to use finite differences the differential equations should be in linear form i.e no variable should have an order  $\geq 2$  and each variable should be independent of the other. That is to say, if the equations are linearized on the basis of a trial solution, the solution of the linearized equation is closer to the correct solution. The new solution is then used as a trial solution for the next iteration and to subsequently obtain a second approximation and this process is repeated until the desired accuracy is obtained. Experience suggests that repetitive calculations or iterations with linearized form of equations frequently converges to the right solution.

The unknown variables are then solved in the radial direction using Newton-Raphson's method of block matrices by using Newman's BAND subroutine. The Newton-Raphson method is a method to find good approximation for the root of a real-valued function. The averaging of time derivatives was solved by using Crank-Nicholson method. The derivatives were solved respect to time by using the halfway point between the old and current time step. At the boundaries a five-point difference approximation is used and at internal boundaries only a three point approximation is used maintaining the accuracy to the order of 2. Newman's method for differentiation in the radial direction consists of collapsing a large sparse matrix into a tri-diagonal matrix.

Central finite difference expressions were used in the domain of the system. In order to maintain accuracy at the boundaries, either a forward or a backward difference was used. Even though internal boundaries have not been considered for the modelling of the anode, it is important to understand the accuracy of the results when a partial cathode model is being implemented along with the anode.

## 7 Results and Discussion

Based off the model and going through time steps, the concentration of hydroxyl ion inside the porous anode continuously decreases (Figure 4).

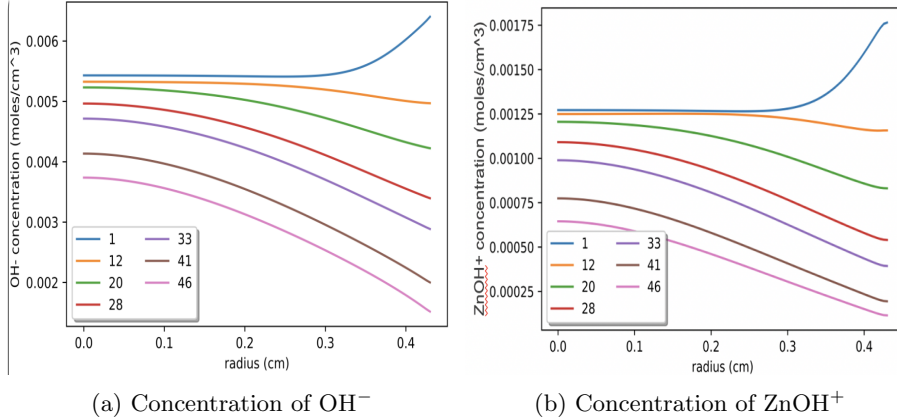


Figure 4

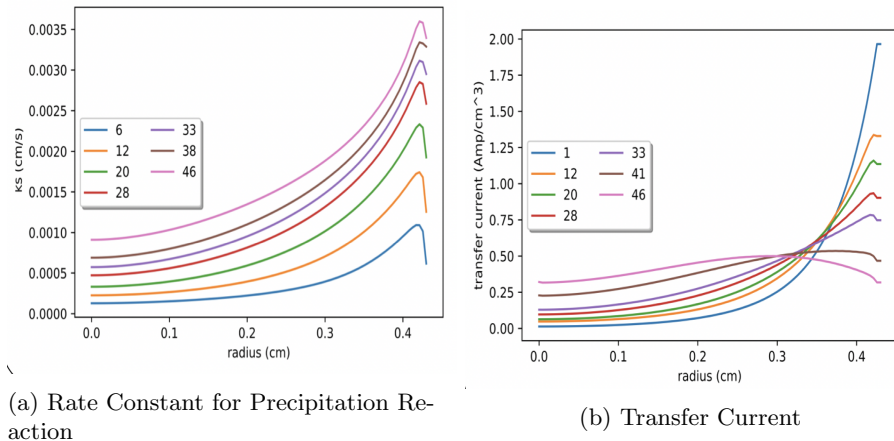


Figure 5

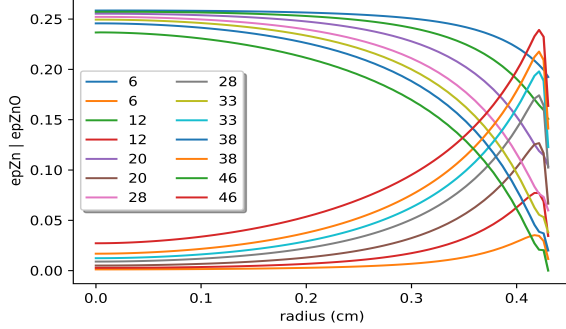


Figure 6: Volume Fraction of Zn and ZnO

Simultaneously, there is an immediate rise of zincate ion due to the dissolution reaction that takes place first. Going through time, the surface zincate ion concentration exceeds its equilibrium value and the precipitation of ZnO starts to occur, as seen in Figure (6). The volume of zinc oxide is relatively large compared to the volume of zinc; therefore, the pores of the anode start to get plugged due to ZnO precipitation. Due to the ZnO deposition leading to the obstruction of the pores, the transfer current starts to shift inwards, as shown in Figure 5(b), i.e., inside the pores since there are hydroxyl ions present inside the pores. However, there is a deficit of hydroxyl ions from the bulk of the electrolyte due to pore plugging. Moreover, as ZnO deposition starts to speed up, the area available for electrochemical reaction to occur decreases and ultimately reaches zero, as observed in Figure 7(a). Simultaneously, the porosity of the anode starts decreasing as shown in Figure 7(b). Eventually, all the hydroxide ions inside the pores reacts, and there isn't anymore zinc area available for electrochemical reaction due to the increased precipitation of ZnO, leading to cell failure.

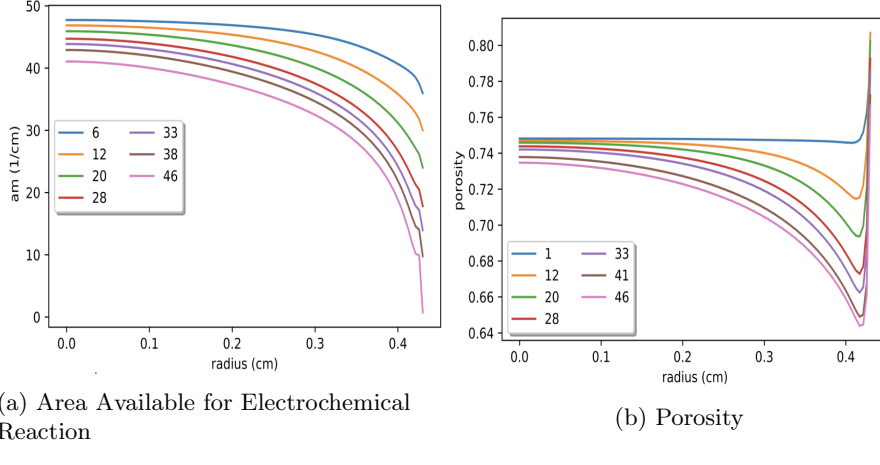


Figure 7

## 8 BAND Algorithm

The system of second order differential equations can be expressed in the form:

where  $i$  is the number of equations and  $k$  is the number of unknowns.

$$F_i = \sum_k a_{i,k}(x) \frac{d^2 C_k}{dx^2} + b_{i,k}(x) \frac{d C_k}{dx} + d_{i,k}(x) C_k - g(x) = 0 \quad [A - 1]$$

This equation can be written for a five point difference approximation where  $j$  is the number of nodal points.

$$\begin{aligned} F_i = & \sum_k Y_{i,k}(j) C_k(j-2) + A_{i,k}(j) C_k(j-1) + B_{i,k}(j) C_k(j) \\ & + D_{i,k}(j) C_k(j+1) + X_{i,k}(j) C_k(j+2) - G(j) = 0 \end{aligned} \quad [A - 2]$$

In order to incorporate the boundary conditions at the two ends of the domain, a forward and a backward finite difference approximation was applied.

$$F_i = \sum_k B_{i,k}(j)C_k(j) + D_{i,k}(j)C_k(j+1) + X_{i,k}(j)C_k(j+2) + X1_{i,k}(j)C_k(j+3) + X2_{i,k}(j)C_k(j+4) - G(j) = 0 \quad [A-4]$$

$$F_i = \sum_k Y2_{i,k}(j)C_k(j-4) + Y1_{i,k}(j)C_k(j-3) + Y_{i,k}(j)C_k(j-2) + A_{i,k}(j)C_k(j-1) + B_{i,k}(j)C_k(j) - G(j) = 0 \quad [A-3]$$

The coefficients of Y2, Y1, Y, A, B, D, X, X1, and X2 are the Jacobian Matrices of the system and G is constant. These values of the Jacobian Matrices are:

**Table A-1. Jacobian Matrices**

Jacobian Matrix	Range	Jacobian	Range
$Y2_{i,k}(j) = \frac{\partial F_i(j)}{\partial C_k(j-4)} _0$	$j = nj;$	$Y2_{i,k}(j) = 0$	$j \leq nj - 1$
$Y1_{i,k}(j) = \frac{\partial F_i(j)}{\partial C_k(j-3)} _0$	$j \geq nj - 1;$	$Y1_{i,k}(j) = 0$	$j < nj - 1$
$Y_{i,k}(j) = \frac{\partial F_i(j)}{\partial C_k(j-2)} _0$	$j \geq 3;$	$Y_{i,k}(j) = 0$	$j < 3$
$A_{i,k}(j) = \frac{\partial F_i(j)}{\partial C_k(j-1)} _0$	$j \geq 2;$	$A_{i,k}(j) = 0$	$j = 1$
$B_{i,k}(j) = \frac{\partial F_i(j)}{\partial C_k(j)} _0$	$all j;$		
$D_{i,k}(j) = \frac{\partial F_i(j)}{\partial C_k(j+1)} _0$	$j \leq nj - 1;$	$D_{i,k}(j) = 0$	$j = nj$
$X_{i,k}(j) = \frac{\partial F_i(j)}{\partial C_k(j+2)} _0$	$j \leq nj - 2;$	$X_{i,k}(j) = 0$	$j > nj - 2$
$X1_{i,k}(j) = \frac{\partial F_i(j)}{\partial C_k(j+3)} _0$	$j \leq 2;$	$X1_{i,k}(j) = 0$	$j > 2$
$X2_{i,k}(j) = \frac{\partial F_i(j)}{\partial C_k(j+4)} _0$	$j = 1;$	$X2_{i,k}(j) = 0$	$j \geq 2$

$G_i(j) = -F_i(j) + \sum_{k=1}^n Y2_{i,k}C_k(j-4) + Y1_{i,k}C_k(j-3) + Y_{i,k}C_k(j-2) + A_{i,k}C_k(j-1) + B_{i,k}C_k(j) + D_{i,k}C_k(j+1) + X_{i,k}C_k(j+2) + X1_{i,k}C_k(j+3) + X2_{i,k}C_k(j+4)$ for all j
--

The system of equations are then written in matrix form, forming a penta-diagonal matrix

$$\begin{pmatrix}
B(1) & D(1) & X(1) & X1(1) & X2(1) & 0 & \dots \\
A(2) & B(2) & D(2) & X(2) & X1(2) & 0 & \dots \\
Y(3) & A(3) & B(3) & D(3) & X(3) & 0 & \dots \\
0 & Y(4) & A(4) & B(4) & D(4) & X(4) & \dots \\
\ddots & \ddots & \ddots & \ddots & \ddots & \ddots & \ddots \\
0 & \dots & Y1(nj-1) & Y(nj-1) & A(nj-1) & B(nj-1) & D(nj-1) \\
0 & \dots & Y2(nj) & Y1(nj) & Y(nj) & A(nj) & B(nj)
\end{pmatrix} \cdot \begin{pmatrix}
C(1) \\
C(2) \\
C(3) \\
C(4) \\
\vdots \\
C(nj-1) \\
C(nj)
\end{pmatrix} = \mathbf{Z}$$

$$\mathbf{Z}$$

$$MT = Z$$

Where M is the Big Matrix consisting of all the Jacobian Matrices. T and Z are the matrices consisting of all the vectors(variables).

The system is solved by decomposing M into an upper and lower triangular coordinate matrix using numpy.coo in python. BAND then solves the matrices using scipy.integrate.essolve giving the values for the variables.

## 9 Conclusion

Further development can be done with this model, mainly by modifying the scripts to do a cathode analysis. In order to maintain accuracy at internal boundaries when the complete cathode model is programmed along with the anode, a five point finite difference approximation with an accuracy of the order  $O(h^4)$  can be used at the external boundaries and in the domain of the system. This is done so that at the internal boundaries, a three-point finite difference approximation can be used with an accuracy of  $O(h^2)$ .

## 10 References

- (1) Podlaha, Elizabeth J. "Theoretical Model of Zinc-Magnaneses Dioxide Alkaline Cells ." 1992, pp. 1–208.
- (2) Fan, D. "Modification of Newman's BAND(J) Subroutine to Multi-Region Systems Containing Interior Boundaries: MBAND." Journal of The Electrochemical Society, vol. 138, no. 6, 1991, p. 1688., doi:10.1149/1.2085854.

(3) Newman, John. NUMERICAL SOLUTION OF COUPLED, ORDINARY DIFFERENTIAL EQUATIONS. Lawrence Berkeley National Laboratory, 1967.